Society For Biomaterials

Modified porous scaffolds of silk fibroin with mimicked microenvironment based on decellularized pulp/fibronectin for designed performance biomaterials in maxillofacial bone defect

Supaporn Sangkert,[1] Suttatip Kamonmattayakul,[2] Wen Lin Chai,[3] Jirut Meesane[1]

[1]Institute of Biomedical Engineering, Faculty of Medicine, Prince of Songkla University, Hat Yai, Songkhla, 90110, Thailand
[2]Department of Preventive Dentistry, Faculty of Dentistry, Prince of Songkla University, Hat Yai, Songkhla, 90110, Thailand
[3]Department of General Dental Practice and Oral and Maxillofacial Imaging, Faculty of Dentistry, University of Malaya, Kuala Lumpur, Malaysia

Received 26 June 2016; revised 2 December 2016; accepted 14 December 2016
Published online 27 March 2017 in Wiley Online Library (wileyonlinelibrary.com). DOI: 10.1002/jbm.a.35983

Abstract: Maxillofacial bone defect is a critical problem for many patients. In severe cases, the patients need an operation using a biomaterial replacement. Therefore, to design performance biomaterials is a challenge for materials scientists and maxillofacial surgeons. In this research, porous silk fibroin scaffolds with mimicked microenvironment based on decellularized pulp and fibronectin were created as for bone regeneration. Silk fibroin scaffolds were fabricated by freeze-drying before modification with three different components: decellularized pulp, fibronectin, and decellularized pulp/fibronectin. The morphologies of the modified scaffolds were observed by scanning electron microscopy. Existence of the modifying components in the scaffolds was proved by the increase in weights and from the pore size measurements of the scaffolds. The modified scaffolds were seeded with MG-63 osteoblasts and cultured. Testing of the biofunctionalities included cell viability, cell proliferation, calcium content, alkaline phosphatase activity (ALP), mineralization and histological analysis. The results demonstrated that the modifying components organized themselves into aggregations of a globular structure. They were arranged themselves into clusters of aggregations with a fibril structure in the porous walls of the scaffolds. The results showed that modified scaffolds with a mimicked microenvironment of decellularized pulp/fibronectin were suitable for cell viability since the cells could attach and spread into most of the pores of the scaffold. Furthermore, the scaffolds could induce calcium synthesis, mineralization, and ALP activity. The results indicated that modified silk fibroin scaffolds with a mimicked microenvironment of decellularized pulp/fibronectin hold promise for use in tissue engineering in maxillofacial bone defects. © 2017 Wiley Periodicals, Inc. J Biomed Mater Res Part A: 105A: 1624–1636, 2017.

Key Words: silk fibroin, bone tissue engineering, scaffolds, microenvironment, mimicking

How to cite this article: Sangkert S, Kamonmattayakul S, Chai WL, Meesane J. 2017. Modified porous scaffolds of silk fibroin with mimicked microenvironment based on decellularized pulp/fibronectin for designed performance biomaterials in maxillofacial bone defect. J Biomed Mater Res Part A 2017:105A:1624–1636.

INTRODUCTION

Currently, there many patients who have critical problems with maxillofacial bone defects from trauma and disease, for instance blast injury, cleft palate, alveolar bone resorption, and oral cancer. In severe cases, those patients need an operation using a biomaterial replacement at the defect area. Therefore, the design of performance biomaterials is a challenge for surgeons and materials scientists.

Tissue engineering of scaffolds is attractive for biomaterial implantation particularly in maxillofacial bone defect. Biodegradable polymers are often fabricated into three dimensional (3D) porous structures to produce bone tissue-engineered scaffolds that are suitable for cell adhesion, proliferation, and regulation. Therefore, the selection of suitable biodegradable polymers is important to create performance biomaterial scaffolds for tissue engineering.

Silk fibroin (SF) is a protein available from the *Bombyx mori* silk worm. Silk fibroin shows performance as a biodegradable polymer. Most of the proteins of the silk include amino acids: glycine (43%), alanine (30%), and serine (12%).[1] These proteins arrange into a crystalline β-sheet form in silk fiber.[1] Silk fibroin shows interesting properties such as slow degradation, biocompatibility, low immunogenicity and toxicity, and good mechanical properties (Young's modulus and tensile strength).[2,3] Silk-based biomaterials as tissue-engineered scaffolds are used increasingly as parts of skeletal tissue like bone cartilage, connective tissue, skin, and ligament.[3] Therefore, in this research, the silk fibroin

Correspondence to: J. Meesane; e-mail: jirutmeesane999@yahoo.co.uk
Contract grant sponsor: The Faculty of Medicine, Prince of Songkla University; contract grant number: EC 56–042-25–2–3

was selected for fabrication into porous scaffolds for maxillofacial bone defects. Nevertheless, to enhance the performance of bone regeneration at the defect area, a silk fibroin porous scaffold needs modification to improve the biological functionality.

Microenvironments are important clues to induce tissue regeneration.[4] Microenvironments were constructed by biological molecules of soluble and insoluble signals.[5] Importantly, microenvironments showed unique biological functionality for cell adhesion, proliferation, migration, and regulation.[4,5] Some literature reported constructed microenvironments for tissue regeneration.[6–8] The literature demonstrated that microenvironments had an effective function to induce tissue regeneration.[9,10] Because of unique biological functionality, a microenvironment was constructed and used in this research to modify biological performance of silk fibroin porous scaffolds.

Decellularized tissue is an important clue to induce tissue regeneration. The literature reported that various types of decellularized tissue were used as a scaffold for tissue regeneration.[11] The decellularized tissue effectively induced tissue regeneration.[12] However, the use of decellularized pulp tissue was rarely reported.[13,14] The components of decellularized pulp tissue are microenvironments that act as clues for tissue regeneration, for instance collagen type I, collagen type II, and fibronectin.[15] Therefore, the microenvironment of decellularized pulp was used for porous scaffolds of silk fibroin.

Fibronectin is one component of the microenvironment. There are many domains that can act as binding sites in this molecule. Fibronectin functions biologically as a binder molecule that can interact with the other components in the microenvironment.[16] Fibronectin acts as a clue to induce cell adhesion, proliferation, and mineralization in bone tissue regeneration.[17] Because of the unique biological functions, fibronectin was selected to use as a component of the microenvironment for modification of silk fibroin porous scaffolds.

The mimicking approach is an attractive method that is used often to create performance scaffolds. Some reports demonstrated that mimicked scaffolds showed the effectiveness to enhance cell adhesion, proliferation, and differentiation.[18–20] The mimicking approach for bone tissue engineering was used for structural and functional mimicking.[21–23] Mimicking the biological performance of scaffolds is an interesting method to create performance scaffolds for bone tissue regeneration. Therefore, in this research, we chose the mimicking approach to create the microenvironment for modification of silk fibroin porous scaffolds.

In this research, constructed porous scaffolds of silk fibroin with the mimicked biological microenvironment based on decellularized pulp/fibronectin was proposed as a designed biomaterial substitute for maxillofacial bone defect. The physical functionality, morphological organization, and biological performance of silk fibroin porous scaffolds were observed and analyzed in this research. The target was to create a performance scaffold that showed promise for use as a biomaterial substitute for maxillofacial bone defects.

TABLE I. Groups of coated silk fibroin scaffolds with different ECMs.

Group	Detail
A	Silk fibroin scaffold
B	Coated silk fibroin scaffold with decellularized pulp
C	Coated silk fibroin scaffold with fibronectin
D	Coated silk fibroin scaffold with decellularized pulp/fibronectin

MATERIALS AND METHODS

Preparation of silk fibroin scaffolds

Degummed silk fibroin was obtained by boiling in 0.02 *M* Na_2CO_3 for 30 min. The silk sericin was removed after rinsing 3 times with distilled water. It was dried in a hot air oven at 60°C for 24 h and the degummed silk fibroin was then dissolved in 9.3 *M* LiBr at 70°C for 3 h.[24] The purified silk fibroin was obtained after dialyzing with distilled water for 3 days.[25] The purified silk fibroin was centrifuged at 3000 rpm at 4°C for 5 min to separate the dregs from the solution. The concentration was adjusted to yield a 3% (w/v) solution and kept at 4°C until further use. The solution was placed in 48-well plates to mold the 3D scaffolds. The freeze drying method was used to fabricate the porous silk fibroin scaffolds. All scaffolds were cut into discs (10 mm diameter × 2 mm thickness).

Modification of silk fibroin scaffolds with mimicked biological microenvironments

In this research, because of the unique biological functionality, fibronectin and decellularized pulp were chosen as the components to mimic microenvironments for bone regeneration. The decellularized pulp was prepared from deciduous teeth that fell out naturally from children who were 6–10 years old and in good health. The parents or guardians of the children gave informed consent and the research was approved by the Research Ethics Committee (REC), Faculty of Dentistry, Prince of Songkla University. The teeth were segmented in half to harvest the pulp tissue which was observed again to confirm that the tissue was disease free. Collagenase and dispase were then used to digest the pulp for 1 h. The solution was separated from the debris using a centrifuge at 37°C and washed 2 times with phosphate-buffered saline (PBS) pH 7.4. The solution was filtered to obtain the decellularized pulp and the freeze-drying process was used for water sublimation.[26]

To modify silk fibroin scaffolds, the decellularized pulp solution was prepared at a concentration of 0.1 mg/mL in 0.1% sodium hypochlorite. Fibronectin solution was prepared at a concentration of 0.1 mg/mL in deionized water.[13,14] A combination of decellularized pulp and fibronectin was prepared at a ratio of 50:50. The 4 groups of solutions are shown in Table I. After soaking the SF scaffolds in each solution for 4 h, they were put in PBS for 30 min before freeze-drying.

Pore size measurement

Scanning electron microscopy (SEM) images of the scaffolds were used for pore size analysis. The pore sizes of the scaffolds in each group were from randomized areas ($n = 25$) to calculate the average pore size. ImageJ software (1.48v, National Institute of Health, Bethesda, MD) was used to measure the pore size in each group.[27]

Weight increase of the scaffolds

The coating deposition of the modified scaffolds in all groups was observed by the weights of the scaffolds before and after coating. The percentage of deposition of the components on the scaffolds from the coating solution was calculated from the following formula.[28]

$$\text{Deposition of components on the scaffold } (w/w,\ \%) = (W_t - W_p)/W_t \times 100\%$$

where W_t is the weight of the modified scaffold and W_p is the weight of scaffold

Scanning electron microscopy (SEM) observation

SEM (Quanta400, FEI, Czech Republic) was used to observe the morphology and characterization of the SF scaffolds that were modified with the solutions. The samples were pre-modified with gold using a gold sputter coating machine (SPI Supplies, Division of Structure Probe, Inc., Westchester, PA).

Cell culturing of MG-63 osteoblasts

MG-63 osteoblasts were seeded in each scaffold with 1×10^6 cells and maintained in an alpha-MEM medium (α-MEM: Gibco®, Invitrogen™, Carlsbad, CA) with the addition of 1% penicillin/streptomycin, 0.1% Fungizone, and 10% fetal bovine serum at 37°C in a humidified 5% CO_2/95% air incubator. The medium was changed every 3–4 days.[29] An osteogenic medium (OS: 20 m*M* *b*-glycerophosphate, 50 μ*M* ascorbic acid, and 100 n*M* dexamethasone; Sigma-Aldrich) was used for osteoblast differentiation of the MG-63 osteoblast cells.[30]

Cell viability (fluorescence microscope on day 3)

The live cells on the scaffold were stained with fluorescein diacetate (FDA, 5 mg/mL acetone). The scaffolds were removed from the media and washed 2 times with PBS. One milliliter of fresh media was added into each scaffold and then 5 μL of the FDA was added into each well and kept in the dark at 37°C for 5 min. The silk scaffold was washed 2–3 times with PBS and observed by fluorescence microscopy.[31]

Cell proliferation assay (PrestoBlue®; days 1, 3, 5, and 7)

PrestoBlue® was used to detect proliferation on days 1, 3, 5, and 7 in each group.[32] The measurement of cell proliferation was performed according to the manufacturer's instructions (PrestoBlue® Cell Viability Reagent, Invitrogen). PrestoBlue® was prepared by mixing with fresh media at a ratio of 1:10 and then added directly into the scaffold and incubated for 1 h at 37°C. The proliferation rate of the cells was measured by monitoring the wavelength absorbance at 600 nm emission.

Calcium content assay

Calcium colorimetric assay (Calcium Colorimetric Assay Kit, BioVision Inc., Milpitas, CA) was used to determine the calcium level secreted from the osteoblast cells. The cells were cultured on SF scaffolds at 7, 14, and 21 days.[33] The cells were then lysed by adding 1% Triton X into each well. The SF scaffolds were frozen at −70°C for 50 min and then thawed at room temperature for 1 h. This was repeated 3 times. The solutions were transferred to Eppendorf tubes and centrifuged at 20,000 rpm for 10 min to remove the supernatant from the pellets.[34] The supernatant (30 μL) was placed in 96-well plates and the volume was adjusted to 50 μL with distilled water. Next 90 μL of a chromogenic reagent and then 60 μL of the Calcium Assay Buffer were added into each well and mixed gently. The reaction was incubated for 5–10 min at room temperature and protected from light. The optical density was measured at 575 nm.

Alkaline phosphatase (ALP) assay

The cells were cultured for 7, 14, and 21 days for the ALP analysis. The SF scaffolds in each group were washed twice with PBS. To extract the cellular proteins, 800 μL of the lysed cell solution (1% Triton X in PBS) was added into each well. The SF scaffolds were frozen at −70°C for 1 hour and then thawed at room temperature for 1 h. This was repeated 3 times. The solutions were transferred to Eppendorf tubes and centrifuged at 20,000 rpm for 10 min to remove the supernatant from the pellets. The alkaline phosphatase Colorimetric Assay Kit (Abcam®, Cambridge, UK) was used to detect the ALP activity of the cells in the SF scaffolds. The phosphatase substrate in the kit used *p*-nitrophenyl phosphate that turned yellow when dephosphorylated by the ALP.

Mineralization assay

Alizarin red staining assay was used for mineralization of the nodules. The alizarin red technique detected calcium deposits on the SF scaffolds in each group. The cells in the SF scaffold were cultured for 14 days and then washed twice with PBS. The cells were fixed with 4% formaldehyde and 1 mL of alizarin red solution (2 g in 100 mL of distilled water and pH adjusted to 4.1–4.3) was added. After 20 min at room temperature in the dark, the alizarin red solution was carefully removed from the SF scaffolds and the SF scaffolds were washed four times with distilled water. Mineralization nodules were observed under a microscope.[35]

Histology

The cell-cultured SF scaffolds were fixed with 4% formaldehyde at 4°C for 24 h and samples were taken on day 5 for cell morphology and on day 14 for detection of calcium. The SF scaffolds in each group were immersed in paraffin and the paraffin sections were cut at 5 μm and placed on a glass slide. The sections were then deparaffinized and hydrated in distilled water. The sample slides were stained in 2 ways. First, hematoxylin and eosin (H&E) stain was used to observe cell migration and adhesion on the SF scaffold.

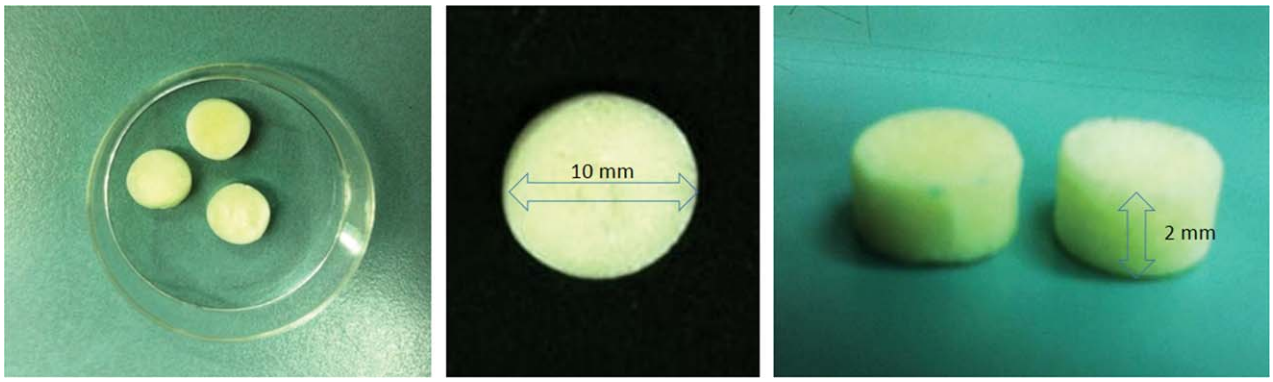

FIGURE 1. Silk fibroin scaffolds after freeze-drying and cut into discs (10 mm diameter × 2 mm thickness).

Second, von Kossa staining was used to detect calcium deposits that were secreted from the osteoblast cells.

Statistical analysis

The samples were measured and statistically compared by one-way ANOVA followed by Tukey's honesty significant difference test (SPSS 16.0 software package). Statistical significance was defined as $*p < 0.05$, and $**p < 0.01$.

RESULTS

Morphological structure observation by scanning electron microscopy

In this research, silk fibroin scaffolds were prepared by the freeze-drying process. The silk fibroin scaffolds were formed into 3D porous scaffolds that were cut into discs (10 mm diameter × 2 mm thickness). The silk fibroin scaffolds were white with a consistent pore size (Fig. 1).

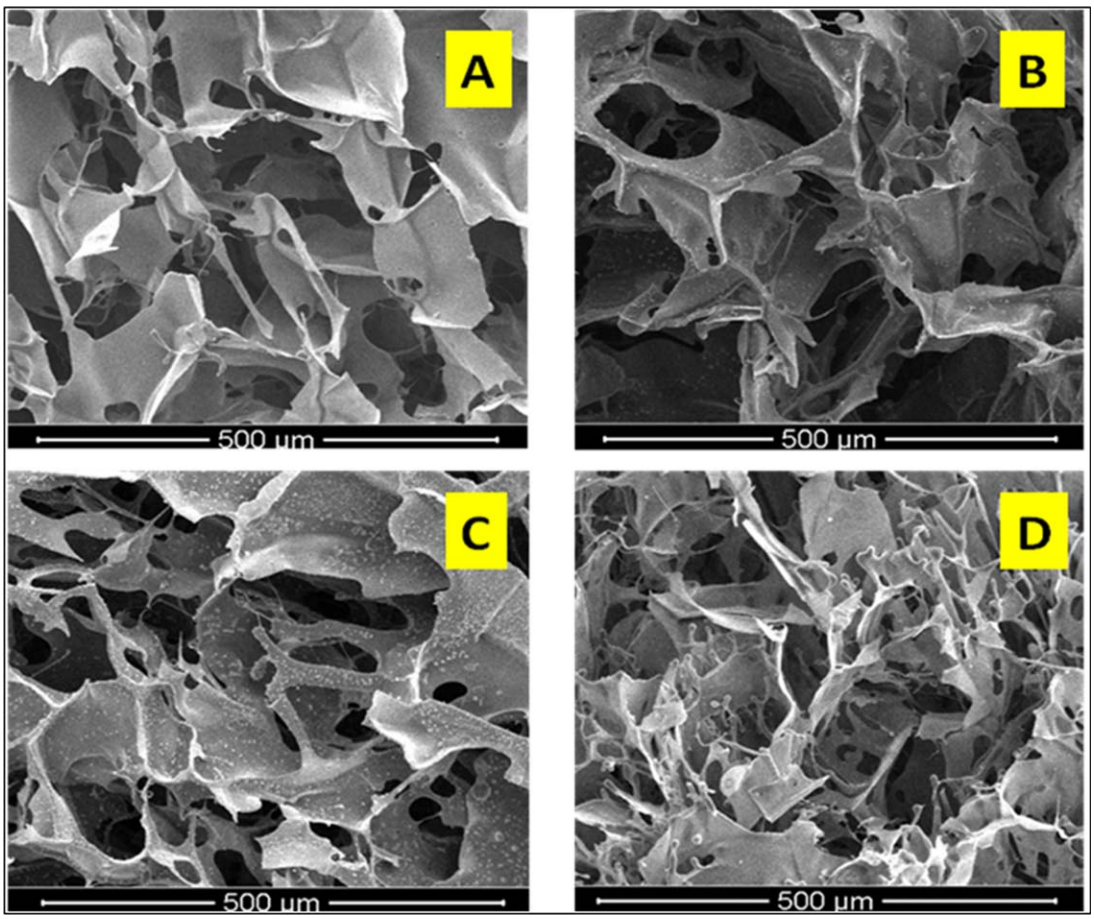

FIGURE 2. SEM images of surface morphology: (A) Silk scaffold, (B) Coated silk fibroin scaffold with decellularized pulp, (C) Coated silk fibroin scaffold with fibronectin, (D) Coated silk fibroin scaffold with decellularized pulp/fibronectin. Scale bar = 500 μm.

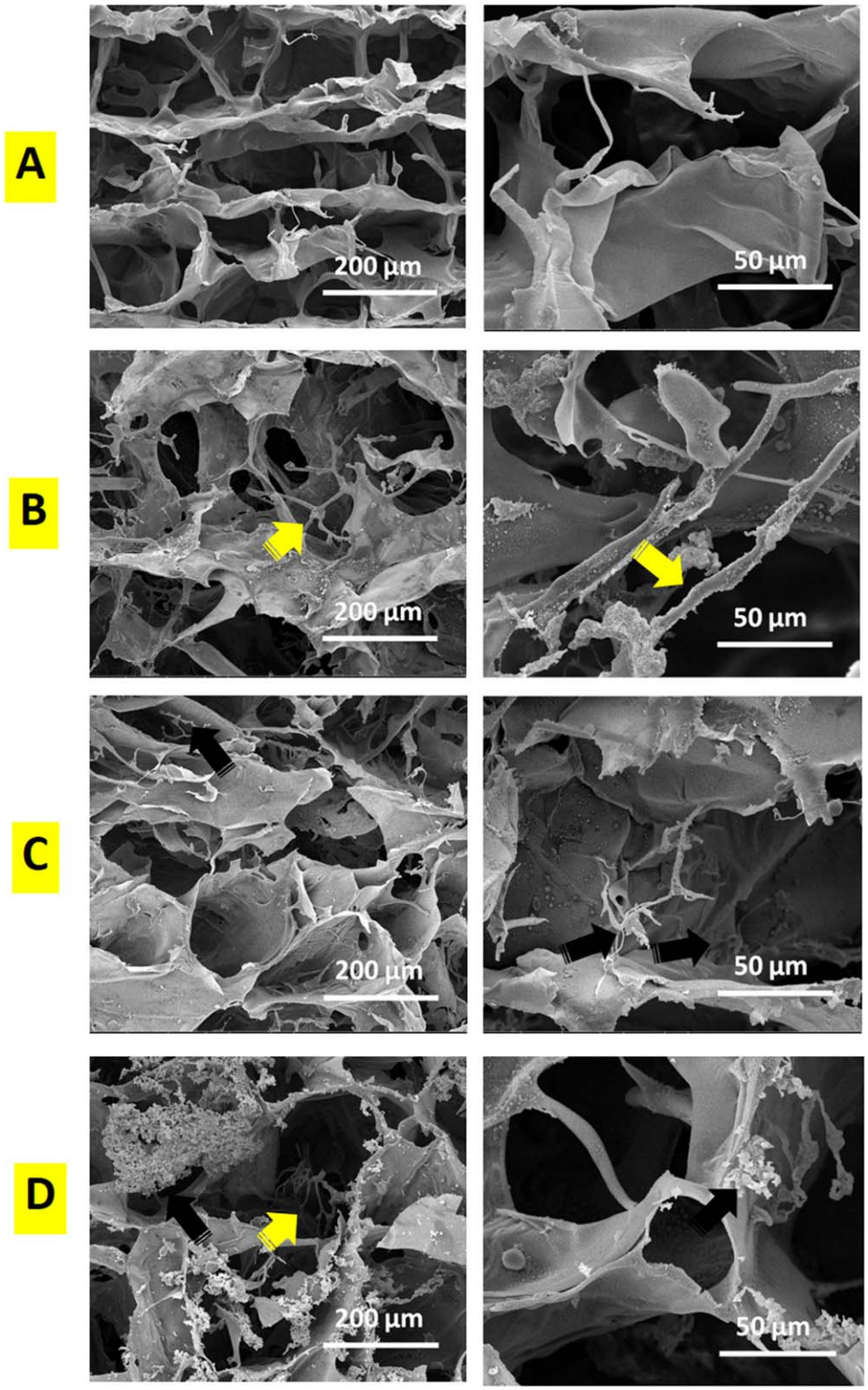

FIGURE 3. SEM images of cross-section morphology: (A) silk scaffolds, (B) coated silk fibroin scaffolds with decellularized pulp, (C) coated silk fibroin scaffolds with fibronectin, (D) coated silk fibroin scaffolds with decellularized pulp/fibronectin; Yellow arrow, rod structure; Black arrow, small fibrillar structure. Scale bar = 200 µm and 50 µm.

The SEM images of the surface of the silk fibroin scaffolds in each group are shown in Figure 2. The surface of the silk fibroin scaffold showed a smooth and porous structure that supported cell adhesion [Fig. 2(A)]. The decellularized pulp showed some small fibrils that covered the surface of the pores in the scaffold [Fig. 2(B)]. In the

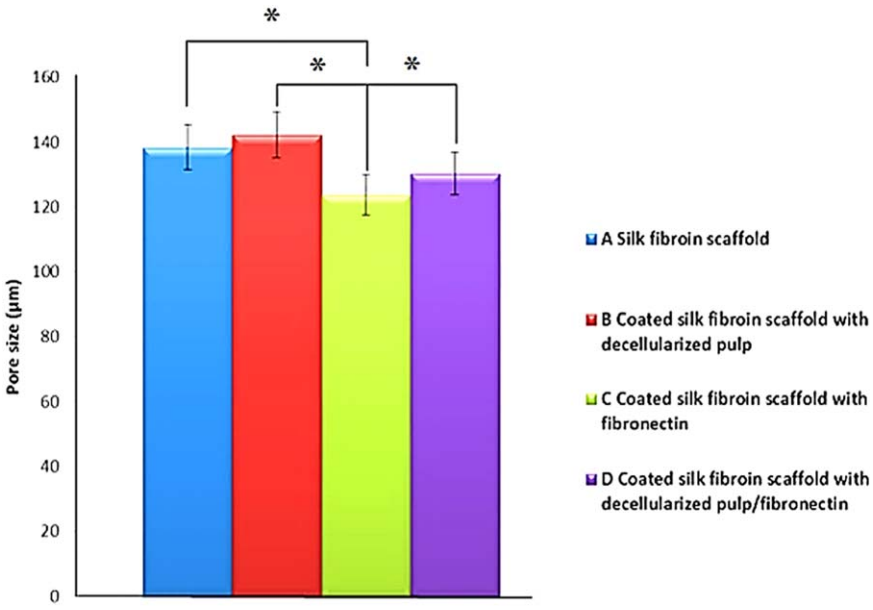

FIGURE 4. The average pore size of scaffold in each group. The symbol (*) represents significant changes (* $p < 0.05$).

case of the modified silk fibroin scaffold with fibronectin, salt crystals covered the surface of the pores in the scaffold [Fig. 2(C)]. Finally, decellularized pulp/fibronectin showed predominant fibers that covered most of the areas of the porous surface [Fig. 2(D)].

The cross-section morphology of the modified silk fibroin scaffolds was observed by SEM (Fig. 3). Smooth surfaces and regular pore sizes were found in the silk fibroin scaffolds [Fig. 3(A)]. In the case of decellularized pulp without fibronectin, the fragments of the fibril structure were attached to the surface and exhibited rough properties on the surface [Fig. 3(B)]. The fibronectins arranged themselves into a small fibrillar structure that adhered to the surface of the pores [Fig. 3(C)]. Finally, the decellularized pulp/fibronectin organized themselves into a fibril structure and an aggregation of salt crystals adhered to the surface [Fig. 3(D)].

The modified silk fibroin scaffolds with decellularized pulp, fibronectin, and decellularized pulp/fibronectin showed fibril structures that were attached in the pores. Those structures appeared on the surface and cross-section morphology of the modified silk fibroin scaffolds.

Pore size analysis of the scaffolds

The scaffolds in all groups showed pore sizes >100 μm. The average pore size of the modified silk fibroin scaffold

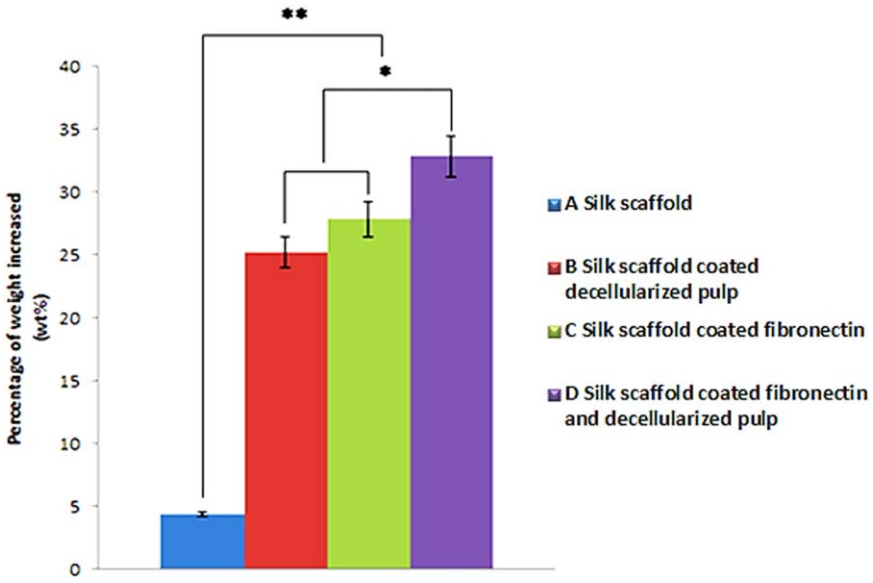

FIGURE 5. Weight increases in percentages of deposition of decellularized pulp, fibronectin, and decellularized pulp/fibronectin. The symbol (*) represents significant changes (*$p < 0.05$), (**$p < 0.01$).

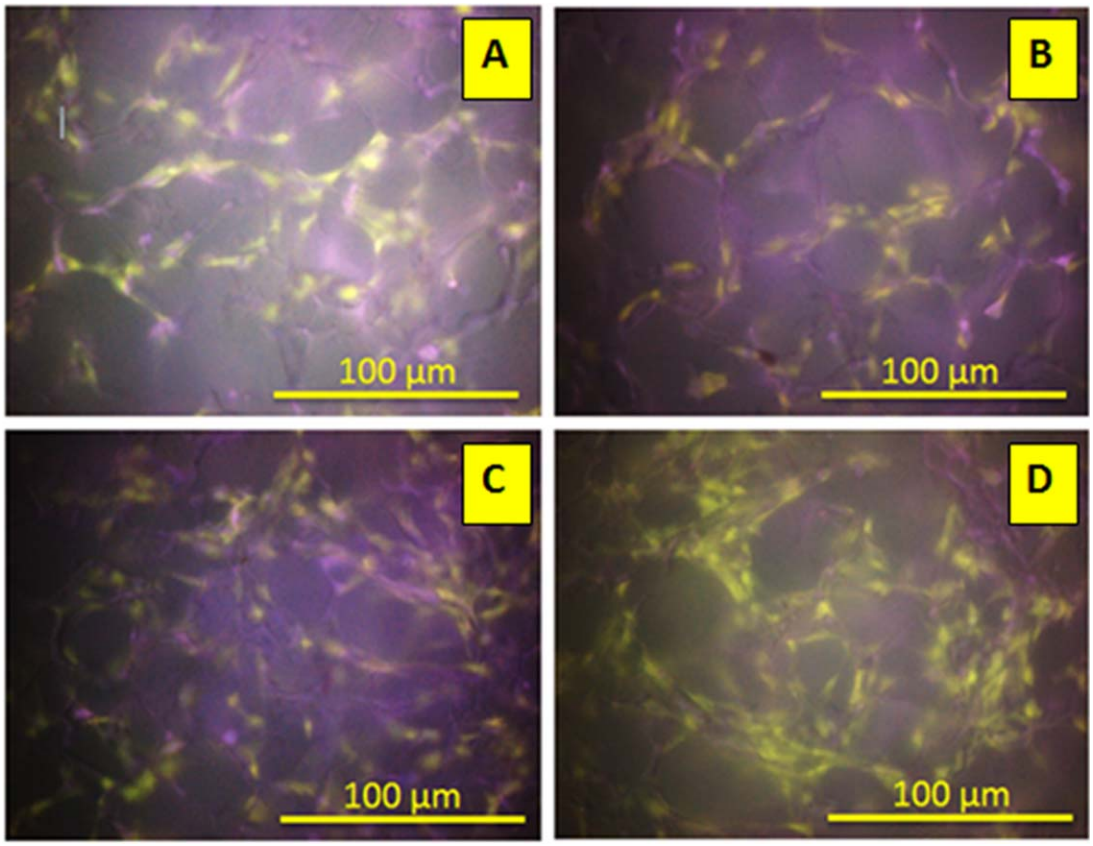

FIGURE 6. FDA cell staining on the scaffold (Green luminance): (A) Silk fibroin scaffold, (B) Coated silk fibroin scaffold with decellularized pulp, (C) Coated silk fibroin scaffold with fibronectin, (D) Coated silk fibroin scaffold with decellularized pulp/fibronectin. Scale bar = 100 µm.

with fibronectin was smaller than the other groups because the small molecules of the fibronectin could infiltrate tightly into the silk fibroin structure to affect the pore size diameter (Fig. 4).

Weight increase of the scaffolds

Confirmation of the existence of decellularized pulp, fibronectin, and decellularized pulp/fibronectin in the silk fibroin scaffolds was performed by an analysis of the increase in

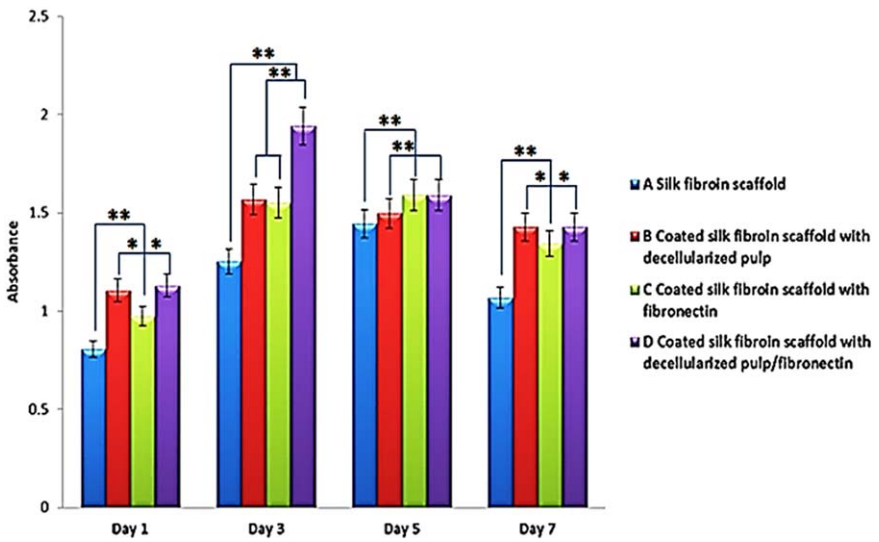

FIGURE 7. Cell proliferations on different silk fibroin scaffold modifying solutions in silk fibroin scaffolds. Cell proliferation was evaluated based on the associative number of metabolically active osteoblast cells in each scaffold group identified by the PrestoBlue® assay. The symbol (*) represents significant changes (*$p < 0.05$), (**$p < 0.01$).

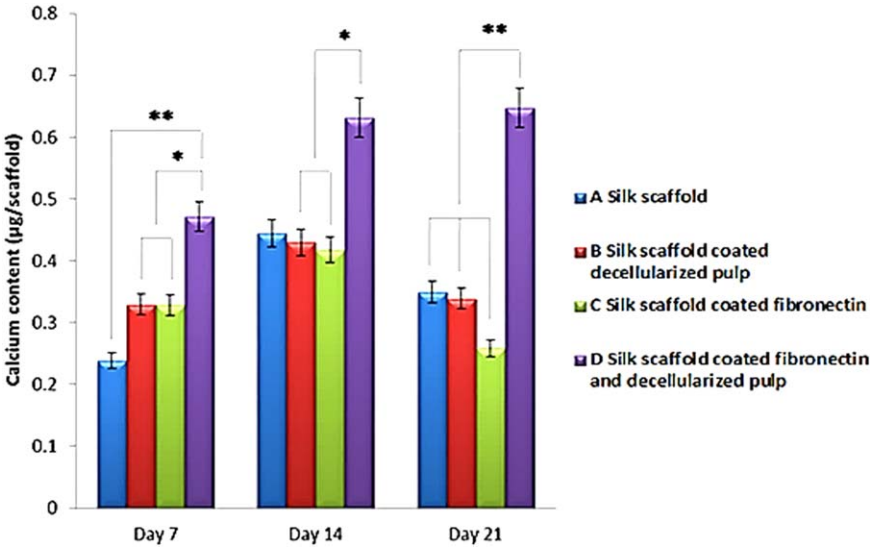

FIGURE 8. The calcium content values in SF scaffolds from MG-63 cell line at days 7, 14, and 21. The symbol (*) represents significant changes (*$p < 0.05$), (**$p < 0.01$).

weights after coating. The modified silk fibroin scaffold with decellularized pulp/fibronectin showed the highest weight increase (Fig. 5). While it appeared that the modified silk fibroin scaffold with decellularized pulp had a lower weight increase than the modified silk fibroin with fibronectin, the difference was not statistically significant.

Cell viability assay

Cell viability was analyzed to demonstrate the performance of the modified silk fibroin scaffolds. A green luminance indicated cell viability on the scaffolds and demonstrated that the MG-63 osteoblast cells could grow in all groups (Fig. 6). The highest efficiency to promote cell proliferation and attachment was demonstrated on the silk fibroin scaffold with decellularized pulp/fibronectin [Fig. 6(D)]. Cell adhesion and spreading in the pores of the modified silk fibroin scaffold with decellularized pulp/fibronectin showed a denser aggregation than the others.

Cell proliferation

Proliferation of the osteoblast cells was evaluated with PrestoBlue® assay on days 1, 3, 5, and 7. Proliferation of the osteoblasts increased continuously from day 1 to day 3 in all groups and reductions were found on days 5 and 7. On day 1, the cell proliferations of the modified silk fibroin scaffold with decellularized pulp, modified silk fibroin scaffold with fibronectin, and modified silk fibroin scaffold with decellularized pulp/fibronectin were significantly higher than the silk fibroin scaffold (Fig. 7). Cell proliferation of the modified silk fibroin scaffold with decellularized pulp/fibronectin was also the highest among the groups on day 3. On day 5, the modified silk fibroin scaffold with fibronectin and modified silk fibroin scaffold with decellularized pulp/fibronectin showed higher efficiencies than the modified silk fibroin scaffold with decellularized pulp and the silk fibroin scaffold, respectively. On day 7, the silk fibroin scaffold clearly indicated a rapid decrease in cell proliferation compared with the other groups.

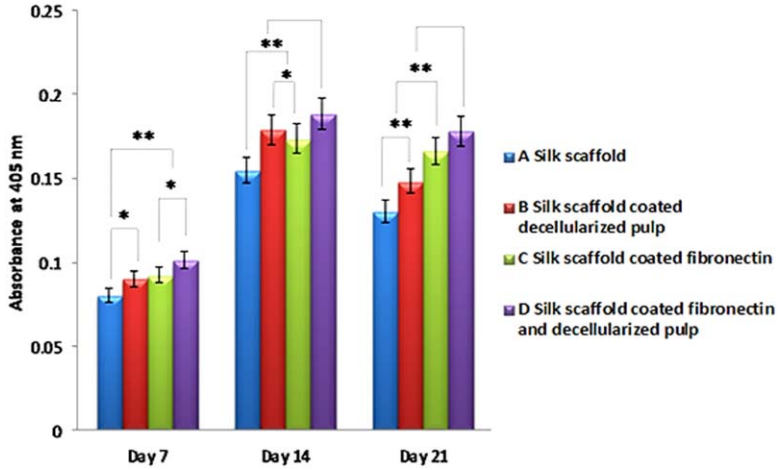

FIGURE 9. ALP activity from MG-63 osteoblast cells on days 7, 14, and 21. The symbol (*) represents significant changes (*$p < 0.05$), (**$p < 0.01$).

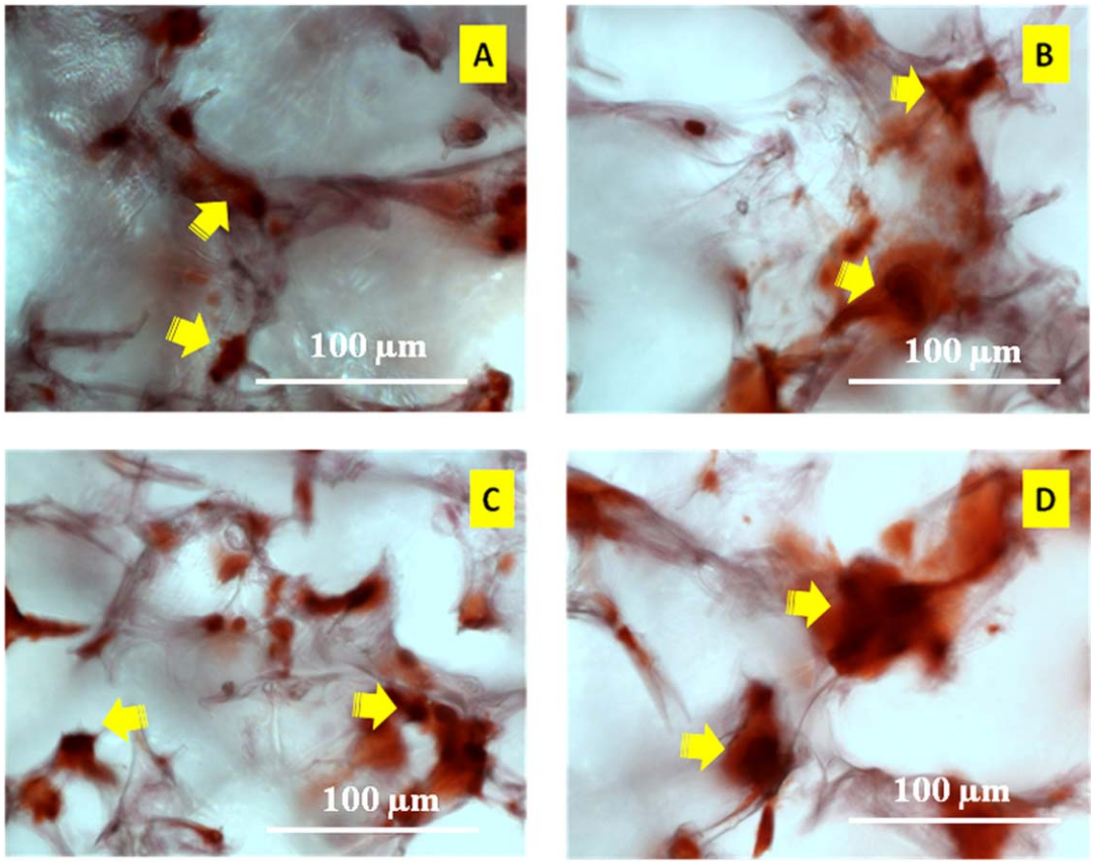

FIGURE 10. Alizarin red staining of SF scaffolds on day 14: (A) Silk fibroin scaffold, (B) Coated silk fibroin scaffold with decellularized pulp, (C) Coated silk fibroin scaffold with fibronectin, (D) Coated silk fibroin scaffold with decellularized pulp/fibronectin. The yellow arrows show the cluster of calcium. Scale bar = 100 μm.

Calcium content analysis

The performance of the modified silk fibroin scaffolds with decellularized pulp/fibronectin was tested with MG-63 osteoblasts. The calcium content was analyzed from the calcium synthesis of the osteoblasts. Mineralization was measured by the matrix calcium content from day 7 to day 21 and tended to show that calcium synthesis progressively increased (Fig. 8). The modified silk fibroin scaffolds with decellularized pulp/fibronectin continued with the highest increase from day 7 to day 21. Interestingly, the decellularized pulp/fibronectin showed higher calcium content than the others at every time point.

Alkaline phosphatase (ALP) activity analysis

The ALP activity analysis measured the quality of the MG-63 osteoblast performance to differentiate the mature cells from the pre-osteoblast cells. All groups of silk fibroin scaffolds revealed a progressive increase in ALP activity from day 7 to 21 (Fig. 9). On day 7, the modified silk fibroin scaffold with decellularized pulp/fibronectin indicated that the MG-63 osteoblasts were osteo-induced and showed the highest ALP activity value. The silk fibroin scaffolds modified with fibronectin showed a higher ALP activity than the modified silk fibroin with decellularized pulp and the silk fibroin scaffolds. On day 14, all groups continued to increase in ALP activity. The modified silk fibroin scaffolds with decellularized pulp had increasingly faster ALP activity than the modified silk fibroin scaffolds with fibronectin and the silk fibroin scaffolds. All of the other scaffolds showed lower ALP activity than the modified silk fibroin scaffolds with decellularized pulp/fibronectin. In the last time period, the modified silk fibroin scaffold with decellularized pulp/fibronectin revealed the highest ALP activity value.

Nodule formation and mineralization analysis

Nodule formation was observed at day 14 after cell seeding. Alizarin red was used to check the osteogenic differentiation state of the cells that can synthesize ECM mineralization. The osteoblast cells showed osteogenesis in all groups of silk fibroin scaffolds (Fig. 10). The red color indicated calcium production from the MG-63 osteoblasts and the calcium deposited on the silk fibroin scaffolds. The results showed red clusters distributed in the scaffolds. Importantly, the MG-63 osteoblast cells could produce calcium in all sample groups. The intensive red clusters in the modified silk fibroin scaffold with decellularized pulp/fibronectin showed the highest amount of deposited calcium.

Histological analysis

Histological analysis was used to observe the morphology and to explain the organization of the cells on the cultured

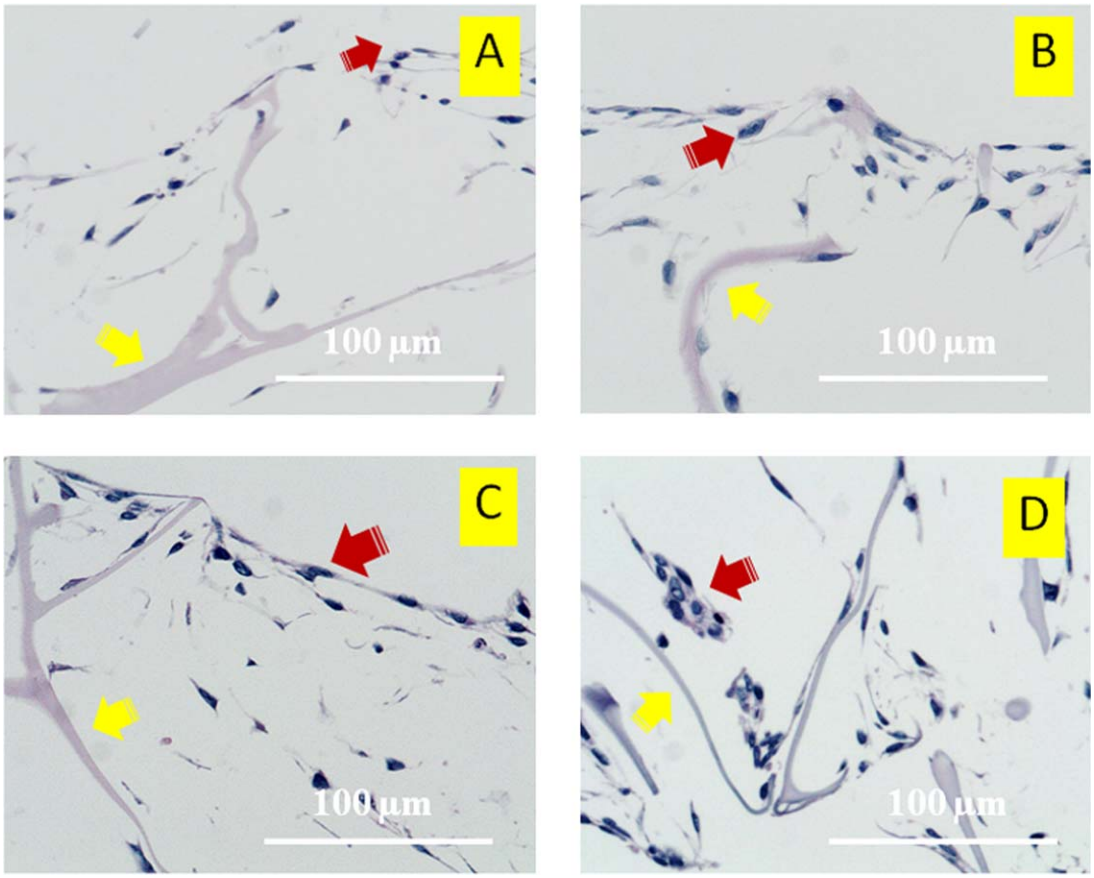

FIGURE 11. Representative histology (H&E) of cross-sections on day 5: (A) Silk fibroin scaffold, (B) Coated silk fibroin scaffold with decellularized pulp, (C) Coated silk fibroin scaffold with fibronectin, (D) Coated silk fibroin scaffold with decellularized pulp/fibronectin; Yellow arrows show the silk scaffold in each group; Red arrows show the osteoblast cells attached to the silk scaffolds in each group. Scale bar = 100 μm.

silk fibroin scaffolds. The MG-63 osteoblast cells could spread thoroughly on the surface of the silk fibroin scaffolds in all groups (Fig. 11). The MG-63 osteoblast cells could attach and migrate into the pores particularly onto the wall surface of the silk fibroin scaffolds. The modified silk fibroin scaffolds with decellularized pulp/fibronectin demonstrated that the cells could attach and spread throughout most of the areas of the scaffold [Fig. 11(D)]. The organization of the cells on the scaffolds from the histological analysis showed similar trends as in Figure 6(D).

von Kossa analysis

von Kossa staining was used to confirm mineralization of the extracellular matrix[35] secreted by the MG-63 osteoblast cells. In all groups of samples, the MG-63 osteoblast cells could proliferate and migrate on the silk fibroin scaffold (Fig. 12). Moreover, the synthesis of calcium-containing salts such as calcium phosphate suggested the behavior of bone regeneration. The black color (yellow arrows) revealed the calcium that was secreted from the MG-63 osteoblast cells and stained by von Kossa. The silk fibroin scaffolds modified with decellularized pulp/fibronectin expressed a lot of osteoblast cells (white arrows) attached to the silk surface [Fig. 12(D)]. The other groups, i.e. silk fibroin scaffold without coating, modified silk fibroin scaffold with decellularized pulp, and modified silk fibroin scaffold with fibronectin, showed both cell attachment and calcium synthesis [Fig. 12(A-C)].

The results of the von Kossa staining indicated that all groups of silk fibroin could induce cell attachment and calcium synthesis. The modified silk fibroin with decellularized pulp/fibronectin showed more cells in the scaffold. Not only could decellularized pulp/fibronectin induce calcium synthesis from the cells, but it could promote cell adhesion.

DISCUSSION

Morphological organization of modified silk fibroin scaffolds

A suitable morphological structure of the scaffolds should promote certain cell behaviors: cell adhesion, proliferation, and migration.[36] In addition, the structures should have connected pores to allow cells to connect with other cells and be suitable for the flow of media in and out of the silk fibroin scaffold.[37–41] It is also necessary to modify the scaffold to enhance the cell behavior and biological performance. Hence, in this research the mimicked microenvironment was added in the pores of the silk fibroin scaffolds to induce biological performance. As previously reported, the fibronectin acted as the binding component in the microenvironment.[42] This indicated that the fibronectin might connect with the

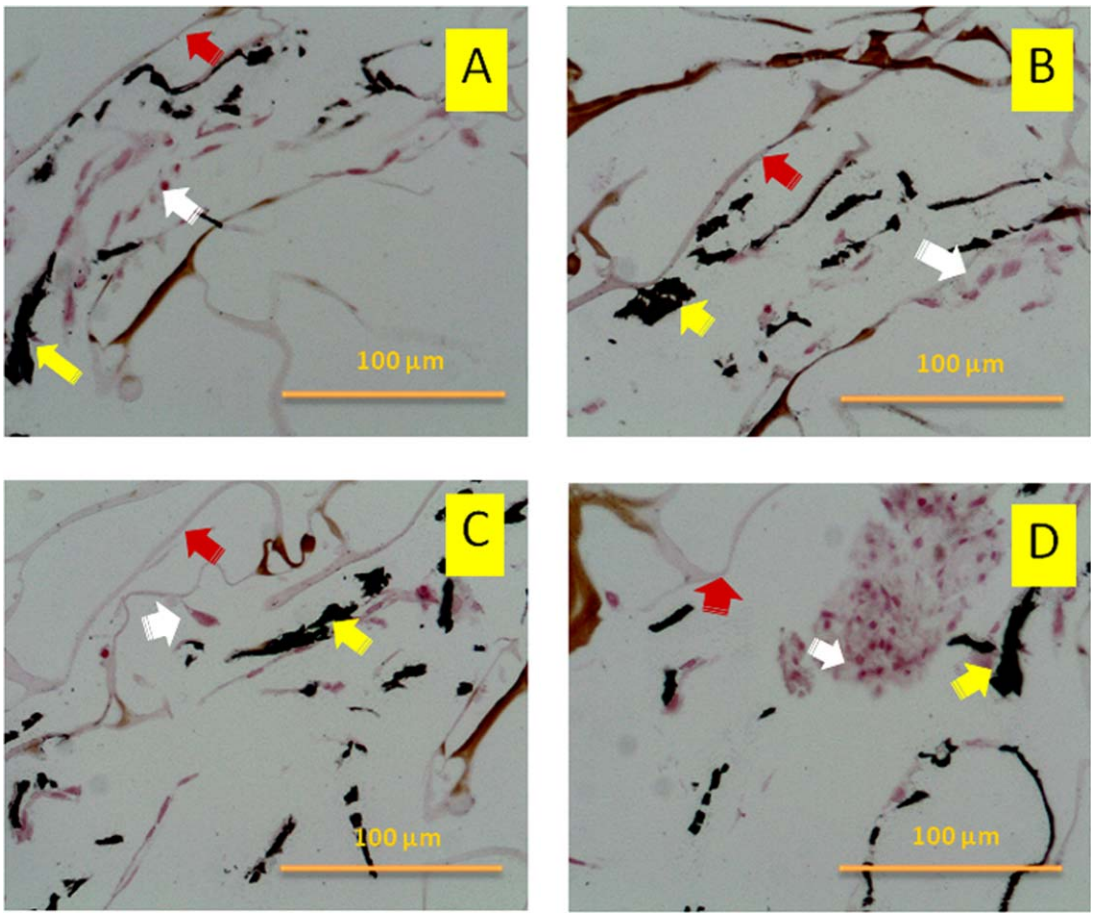

FIGURE 12. Histological sections of scaffold structures stained with von Kossa after day 14: (A) Silk fibroin scaffold, (B) Coated silk fibroin scaffold with decellularized pulp, (C) Coated silk fibroin scaffold with fibronectin, (D) Coated silk fibroin scaffold with decellularized pulp/fibronectin; White arrows, osteoblasts in scaffold; Yellow arrows, clusters of calcium; Red arrows, scaffold. Scale bar = 100 µm.

fragments of microenvironment via specific and non-specific binding.[42] According to this unique function, fibronectin plays the role of reconstructing the microenvironment fragments of decellularized pulp. Therefore, the mimicked biological microenvironment of decellularized pulp/fibronectin organized themselves into a more complicated structure than the

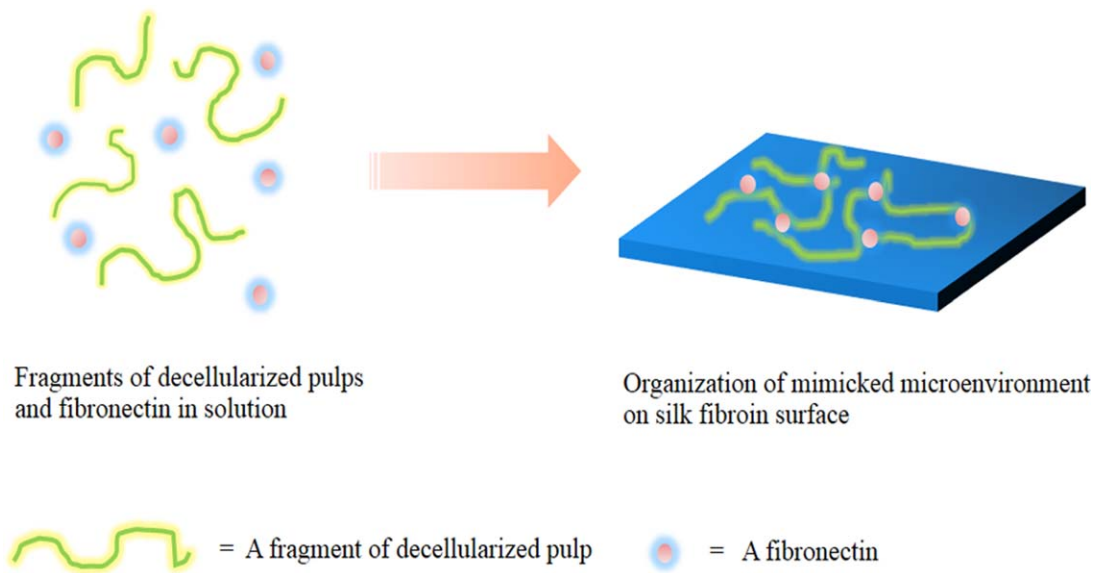

FIGURE 13. Proposed construction of mimicked microenvironment adhering to the surface of the silk fibroin scaffold.

decellularized pulp or fibronectin. As a mimicked microenvironment of decellularized pulp/fibronectin, small fibrils could form and adhere to the surface of the pores of the silk fibroin scaffolds. The proposed mimicked microenvironment of decellularized pulp/fibronectin is shown in Figure 13. This mimicked microenvironment plays the important role of promoting cell adhesion and proliferation that leads to tissue regeneration.[43,44] This research indicated that the complicated structure of the mimicked microenvironment could act as the clue to induce bone tissue regeneration.

Physical structure of modified silk fibroin scaffolds

A suitable pore size in the cell culture systems for cell migration should be larger than 100 μm with interconnective pores.[45] In this research, the porous structures of the non-modified and modified silk fibroin scaffolds showed suitable sizes for osteoblast residence and migration.[46] Notably, the pore sizes were not significantly different The smaller pore size of the modified silk fibroin scaffold with fibronectin might come from the fibronectin that could penetrate and spread in the pores and adhere to those pores that led to a decreased pore size. Interestingly, the significantly increased weight of the modified silk fibroin scaffolds implied that the decellularized pulp and fibronectin could adhere and organize themselves inside the pores.

Biological performance of modified silk fibroin scaffolds

The report demonstrated that silk fibroin scaffolds needed special modifications to enhance the biological performance to induce the formation of bone tissue.[47] Therefore, modified silk fibroin scaffolds with decellularized pulp and fibronectin were presented in this research. The aim of modification is to mimic the microenvironment of decellularized pulp/fibronectin that can enhance the biological performance of silk fibroin scaffolds such as cell adhesion and proliferation. The dense aggregation of cell adhesion in the pores might be from the mimicked biological microenvironment that could induce cell aggregation.[48] Obviously, a combination of decellularized pulp and fibronectin could stimulate cell proliferation and attachment because dental pulp contains proteoglycans and glycosaminoglycans, for example, fibronectin, and different types of collagen.[45] Microenvironments have important roles to play in cell proliferation.[49] A previous study used decellularized tissue as a scaffold to demonstrate the unique function on cell proliferation and differentiation.[50]

In this research, the results from the calcium content and mineralization analyses demonstrated that the mimicked biological microenvironment of decellularized pulp/fibronectin played a role as a clue to induce calcium synthesis. The results of the ALP analysis indicated that the mimicked biological microenvironment of decellularized pulp/fibronectin could induce the osteo-induction of preosteoblasts to a mature stage. This cell behavior might have come from two reasons. First, the fibronectin induced cell adhesion, extension, and migration adsorption of the osteoblasts.[51] Second, the decellularized pulp has many components of the microenvironment which include collagen, fibronectin, and versican which acted as important clues for MG-63 osteoblasts to induce tissue regeneration.[52] Therefore, the mimicked biological microenvironment of decellularized pulp/fibronectin in this research showed its role as an important clue for bone tissue engineering.

CONCLUSIONS

Modified silk fibroin scaffolds with mimicked microenvironment of decellularized pulp/fibronectin were proposed as a biomaterial to replace a bone defect at the maxillofacial area. The results demonstrated that the mimicked microenvironment could attach to the pore walls of the silk fibroin scaffolds. The mimicked biological microenvironment organized into a fibril structure. Obviously, modified silk fibroin scaffolds with mimicked microenvironment based on decellularized pulp/fibronectin played an important role as a clue to induce cell adhesion, proliferation, and calcium synthesis which can lead to promotion of bone tissue regeneration. The predominant biological performance of a modified silk fibroin scaffold with mimicked biological microenvironment of decellularized pulp/fibronectin holds promise as a scaffold to replace bone defects at maxillofacial area. Nevertheless, to prove the biological performance, the scaffolds need *in vivo* or *ex vivo* testing. Furthermore, mimicked microenvironments based on other types of decellularized tissue are attractive alternatives to modify porous scaffolds in future work.

ACKNOWLEDGMENTS

Many thanks to the Institute of Biomedical Engineering and Queen Sirikit Sericulture Centre in Narathiwat for the supply of the silk.

REFERENCES

1. Zhao Z, Li Y, Xie MB. Silk fibroin-based nanoparticles for drug delivery. Int. J. Mol. Sci 2015; 16:4880–4903.
2. Kearns V, MacIntosh AC, Crawford A, Hatton PV. Silk-based biomaterials for tissue Engineering. Top Tissue Eng 2008;4:1–19.
3. Wang Y, Blasioli DJ, Kim HJ, Kim HS, Kaplan DL. Cartilage tissue engineering with silk scaffolds and human articular chondrocytes. Biomaterials 2006; 27:4434–4442.
4. Rice JJ, Martino MM, De Laporte L, Tortelli F, Briquez PS, Hubbell JA. Engineering the Regenerative Microenvironment with Biomaterials. Adv Healthc Mater 2013;2:57–71.
5. Lutolf MP, Hubbell JA. Synthetic biomaterials as instructive extracellular microenvironments for morphogenesis in tissue engineering. Nat Biotechnol 2005;23:47–55.
6. Burdick JA, Vunjak-Novakovic G. Engineered microenvironments for controlled stem cell differentiation. Tissue Eng Part A 2009;15: 205–219.
7. Wray LS, Orwin EJ. Recreating the Microenvironment of the Native Cornea for Tissue Engineering Applications. Tissue Eng Part A 2009;5:1463–1472.
8. Dua F, Wanga H, Zhaoa W, Lia D, Konga D, Yanga J, Zhang Y. Gradient nanofibrous chitosan/poly ε-caprolactone scaffolds as extracellular microenvironments for vascular tissue engineering. Biomaterials 2012;33:762–770.
9. Nuttelmana CR, Ricea MA, Rydholma AE, Salinasa CN, Shaha DN, Anseth KS. Macromolecular monomers for the synthesis of hydrogel niches and their application in cell encapsulation and tissue engineering. Prog Polym Sci 2008;33:167–179.
10. Lund AW, Yener B, Stegemann JP, Plopper GE. The natural and engineered 3D microenvironment as a regulatory cue during stem cell fate determination. Tissue Eng Part B 2009;15:371–380.

11. Gilberta TW, Sellaroa TL, Badylak SF. Decellularization of tissues and organs. Biomaterials 2006;27:3675–3683.
12. Flynn LE. The use of decellularized adipose tissue to provide an inductive microenvironment for the adipogenic differentiation of human adipose-derived stem cells. Biomaterials 2010;31:4715–4724.
13. S, Sangkert J, Meesane S, Kamonmattayakul WL. Chai Modified silk fibroin scaffolds with collagen/decellularized pulp for bone tissue engineering in cleft palate: Morphological structures and biofunctionalities. Mater Sci Eng C 2016;58:1138–1149.
14. Sangkert S, Kamonmattayakul S, Chai WL, Meesane J. A biofunctional-modified silk fibroin scaffold with mimic reconstructed extracellular matrix of decellularized pulp/collagen/fibronectin for bone tissue engineering in alveolar bone resorption. Mater Lett 2016;166:30–34.
15. Miyagi SPH, Kerkis I, da Costa Maranduba CM, Gomes CM, Martins MD, Marques MM. Expression of extracellular matrix proteins in human dental pulp stem cells depends on the donor tooth conditions. J Endod 2010; 36:826–831.
16. Mao Y, Schwarzbauer JE. Fibronectin fibrillogenesis, a cell-mediated matrix assembly process. Matrix Biol 2005;24:389–399.
17. Lee JS, Yang JH, Hong JY, Jung UW, Yang HC, Lee IS, Choi SH. Early bone healing onto implant surface treated by fibronectin/oxysterol for cell adhesion/osteogenic differentiation: In vivo experimental study in dogs. J Periodontal Implant Sci 2014;44:242–250.
18. Ma PX. Biomimetic materials for tissue engineering. Adv Drug Deliv Rev 2008;60:184–198.
19. Shin H, Jo S, Mikos AG. Biomimetic materials for tissue engineering. Biomaterials 2003;24:4353–4364.
20. Kim TG, Shin H, Lim DW. Biomimetic scaffolds for tissue engineering. Adv Funct Mater 2012;22:2446–2468.
21. Wu C, Zhou Y, Fan W, Han P, Chang J, Yuen J, Zhang M, Xiao Y. Hypoxia-mimicking mesoporous bioactive glass scaffolds with controllable cobalt ion release for bone tissue engineering. Biomaterials 2012;33:2076–2085.
22. Lu ZF, Roohani-Esfahani S-I, Wang G, Zreiqat H. Bone biomimetic microenvironment induces osteogenic differentiation of adipose tissue-derived mesenchymal stem cells. Nanomed: Nanotechnol Biol Med 2012;8:507–515.
23. Liu X, Smith LA, Hua J, Ma PX. Biomimetic nanofibrous gelatin/apatite composite scaffolds for bone tissue engineering. Biomaterials 2009;30:2252–2258.
24. Chang G, Kim HJ, Kaplan D, Vunjak-Novakovic G, Kandel RA. Porous silk scaffolds can be used for tissue engineering annulus fibrosus. Eur Spine J 2007;16:1848–1857.
25. Zhao Y, Legeros RZ, Chen J. Initial study on 3D porous silk fibroin scaffold: Preparation and morphology. Bioceram Dev Appl 2011;1: 1–3.
26. Traphagen SB, Fourligas N, Xylas J, Sengupta S, Kaplan D, Georgakoudi I, Yelick PC. Characterization of natural, decellularized and reseeded porcine tooth bud matrices. Biomaterials 2012; 33:5287–5296.
27. Kasoju N, Kubies D, Kumorek MM, Krız J, Fabryova E, Machova L, Kovarova J, Rypacek F. Dip TIPS as a facile and versatile method for fabrication of polymer foams with controlled shape size and pore architecture for bioengineering applications. PLoS ONE 2014;9:1–16.
28. He P, Sahoo S, Ng KS, Chen K, Toh SL, Goh JCH. Enhanced osteoinductivity and osteoconductivity through hydroxyapatite coating of silk-based tissue-engineered ligament scaffold. Biomed Mater Res Part A 2013;101:A555–566.
29. Liu X, Zhao M, Lu J, Ma J, Wei J, Wei S. Cell responses to two kinds of nanohydroxyapatite with different sizes and crystallinities. Int J Nanomedicine 2012;7:1239–1250.
30. Kim BS, Kang HJ, Lee J. Improvement of the compressive strength of a cuttlefish bone-derived porous hydroxyapatite scaffold via polycaprolactone coating. J Biomed Mater Res Part B: Appl Biomater 2013;101:1302–1309.
31. Li TT, Ebert K, Vogel J, Groth T. Comparative studies on osteogenic potential of micro- and nanofibre scaffolds prepared by electrospinning of poly(ϵ-caprolactone). Prog Biomater 2013;13: 1–13.
32. Liu H, Xia L, Dai Y, Zhao M, Zhou Z, Liu H. Fabrication and characterization of novel hydroxyapatite/porous carbon composite scaffolds. Mater Lett 2011;66:36–38.
33. Kim SE, Song SH, Yun YP, Choi BJ, Kwon K, Bae MS, Moon HJ, Kwon YD. The effect of immobilization of heparin and bone morphogenic protein-2 (BMP-2) to titanium surfaces on in flammation and osteoblast function. Biomaterials 2010;32:1–8.
34. Ji H. Lysis of cultured cells for immunoprecipitation. Cold Spring Harb Lab Protoc 2010;2010:1–5.
35. Wang YH, Liu Y, Maye P, Rowe DW. Examination of mineralized nodule formation in living osteoblastic cultures using fluorescent dyes. Biotechnology 2006;22:1697–1701.
36. Rigogliuso S, Pavia FC, Brucato V, La Carrubba V, Favia P, Intranuovo F, Gristina R, Ghersi G. Use of modified 3D scaffolds to improve cell adhesion and drive desired cell responses. Ital Assoc Chem Eng 2012;27:415–420.
37. Sun W, Shao Z, Ji J. Particle-assisted fabrication of honeycomb-structured hybrid films via breath figures method. Polymer 2011; 51:4169–4175.
38. Nikkhah MF, Manoucheri ES, Khademhosseini A. Engineering microscale topographies to control the cell-substrate interface. Biomaterials 2012;33:5230–5246.
39. Ho MH, Kuo PY, Hsieh HJ, Hsien TY, Hou LT, Lai JY, Wang DM. Preparation of porous scaffolds by using freeze-extraction and freeze-gelation methods. Biomaterials 2004;25:129–138.
40. Don TM, Hsu YC, Tai HY, Fu EM, Cheng LP. Preparation of bicontinuous macroporous polyamide copolymer membranes for cell culture. J Membr Sci 2012;145-146:784–792.
41. Rath SN, Strobel LA, Arkudas A, Beier JP, Maier AK, Greil P, Horch RE, Kneser U. Osteoinduction and survival of osteoblasts and bone-marrow stromal cells in 3D biphasic calcium phosphate scaffolds under static and dynamic culture conditions. J Cell Mol Med 2012;16:2350–2361.
42. Halper J, Kjaer M. Basic components of connective tissues and extracellular matrix: Elastin, fibrillin, fibulins, fibrinogen, fibronectin, laminin, tenascins and thrombospondins. Adv Exp Med Biol 2014;802:31–47.
43. Mason BN, Califano JP, Reinhart-King CA. Matrix stiffness: A regulator of cellular behavior and tissue formation. Eng Biomater Regen Med 2011;19–37.
44. Hoshiba T, Chen G, Endo C, Maruyama H, Wakui M, Nemoto E, Kawazoe N, Tanaka M. Decellularized extracellular matrix as an in vitro model to study the comprehensive roles of the ECM in stem cell differentiation. Stem Cells Int 2015;1–10.
45. Linde A. The extracellular matrix of the dental pulp and dentin. J Dent Res 1985;64:523–529.
46. Mantila Roosa SM, Kemppainen JM, Moffitt EN, Krebsbach PH, Hollister SJ. The pore size of polycaprolactone scaffolds has limited influence on bone regeneration in an in vivo model. J Biomed Mater Res Part A 2010;92A:2010.
47. Moisenovich MM, Yu. Arkhipova A, Orlova AA, Drutskaya MS, Volkova SV, Zacharov SE, Agapov II, Kirpichnikov MP. Composite scaffolds containing silk fibroin, gelatin, and hydroxyapatite for bone tissue regeneration and 3D cell culturing. Acta Nat 2014;6:96–101.
48. Pati F, Jang J, Ha DH, Kim SW, Rhie JW, Shim JH, Cho DW. Printing three-dimensional tissue analogues with decellularized extracellular matrix bioink. Nat Commun 2014;5:1–11.
49. Hirst SJ, Twort CH, Lee TH. Differential effects of extracellular matrix proteins on human airway smooth muscle cell proliferation and phenotype. Am J Respir Cell Mol Biol 2000;23:335–344.
50. Crapo PM, Gilbert TW, Badylak SF. An overview of tissue and whole organ decellularization processes. Biomaterials 2011;32:3233–3243.
51. Rivera-Chacon DM, Alvarado-Velez M, Acevedo-Morantes CY, Singh SP, Gultepe E, Nagesha D, Sridhar S, Ramirez-Vick JE. Fibronectin and vitronectin promote human fetal osteoblast cell attachment and proliferation on nanoporous titanium surfaces. J Biomed Nanotechnol 2013;9:1092–1097.
52. Goldberg M, Smith J. Cells and extracellular matrices of dentin and pulp: A biological basis for repair and tissue engineering. Crit Rev Oral Biol Med 2004;15:13–27.